

Remarks on low-mass pseudoscalar-pseudoscalar dynamics including the S -wave $I = 1$ KK system

John Weinstein

Department of Physics, University of Mississippi, University, Mississippi 38677

(Received 22 May 1992)

We discuss the relative importance of several possible hadron-hadron interaction mechanisms and review a coupled-channel Schrödinger model incorporating some of these mechanisms. Its application to pseudoscalar-pseudoscalar S -wave scattering is reviewed and updated to include new insights about the underlying intermeson interactions. We find that s -channel resonance formation and quark-exchange processes are sufficient to reproduce experimental observations, and that the new predictions are qualitatively consistent with the earlier results. New results for exotic K^+K^+ scattering are also presented and compared with a Born-level quark-exchange calculation.

PACS number(s): 13.75.Lb, 12.40.Aa

INTRODUCTION

A common approach to modeling hadron-hadron interactions is to sum the effects of both s -channel and t -channel meson exchange. Another possible interaction mechanism is quark exchange between two nearby hadrons. In several earlier papers we presented results based on a combination of quark-exchange and s -channel resonance interactions (in those isospin and strangeness sectors where such s -channel resonances exist) for all S -wave pseudoscalar-pseudoscalar (PP) systems [1–3] except the exotic KK systems which we report on here.

Quark-exchange interactions have recently been studied in systems of S -wave vector-vector states by Dooley, Swanson, and Barnes using the Born approximation and calculating phase shifts and effective meson-meson potentials [4]. These techniques have also been applied by Barnes and Swanson [5] to single channel $\pi^+\pi^+$ and K^+K^+ systems, and they suggest that certain assumptions in our earlier coupled channel studies are not appropriate.

In this paper we first discuss the differences between t -channel meson exchange and quark exchange, and show that quark-exchange diagrams represent new physics. We then apply the insights of the Born-approximation work to the coupled-channel analysis presented earlier, and show that the formalism developed there survives the suggested modifications. Finally, we show predictions for the unmeasured K^+K^+ phase shift and cross section, and compare these results with the Born-approximation calculations of Barnes and Swanson [5].

HADRON-HADRON INTERACTIONS

When two scattering hadrons are within a few fm of each other they may interact via the strong force, but the mechanisms driving their interactions are still not well understood. One idea, dating back to Yukawa [6], is that the interaction takes place via t -channel meson exchange as depicted in Fig. 1(a) for the specific case of meson-

meson (MM) scattering. The S matrix for hadron-hadron scattering may be formally determined by summing over the exchange of all allowed intermediate mesons. The range of these interactions is, however, dependent on the mass m of the exchanged meson, and is of the order of the Compton wavelength $\lambda = \hbar/mc$. The Compton wavelength of the π is about 1.4 fm, but for the next lightest pseudoscalar mesons, the K and the η , $\lambda_K = 0.4$ fm and $\lambda_\eta = 0.36$ fm. The lightest vector meson is the ρ and $\lambda_\rho = 0.26$ fm. Thus, when two scattering hadrons, whose individual wave functions are significant over ranges of about 1 fm, are close enough to scatter via meson ex-

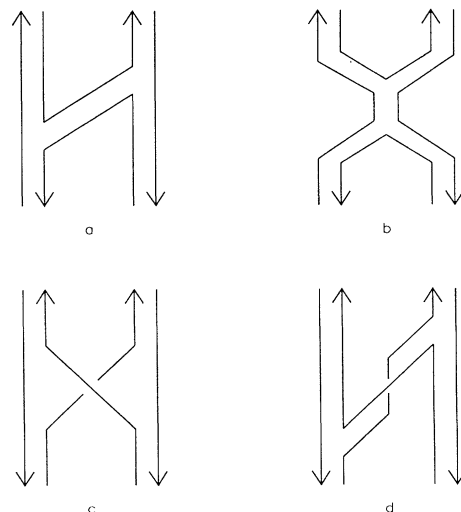


FIG. 1. Quark line diagrams of several possible interaction mechanisms in meson-meson scattering; (a) t -channel meson exchange, (b) s -channel resonances, and (c) quark exchange. In (d) we show a quark-exchange process deformed by having a quark line scatter backwards and forwards in time.

change, they are, with the exception of π exchange, overlapping. It follows that the whole picture of meson-exchange interactions between pointlike hadrons loses much of its justification when applied to physical hadrons.

The picture of overlapping-hadron wave functions, which undermines the meson-exchange picture, suggests two other interaction mechanisms. One is due to $q\bar{q}$ -annihilation and creation processes, depicted in Fig. 1(b) for MM scattering, which occurs when a quark in one meson annihilates with an antiquark in the other meson. This leads to the production of an s -channel meson, and the S matrix can again be determined by summing over all s -channel resonances. The duality of s - and t -channel meson exchange for MM scattering is evident from Figs. 1(a) and 1(b), which may be continuously deformed into one another. Thus, the S matrix can be described in terms of a complete set of either process; considering subsets of both processes runs the risk of unphysical predictions due to double counting.

Another possible interaction mechanism is quark exchange [Fig. 1(c)] between two nearby scattering hadrons whose wave functions overlap. If there are identical particles in the scattering hadrons the complete wave function of the system must, in fact, contain such diagrams in order to be antisymmetrized. Hence the dynamics of quark exchange are intrinsic to the dynamics of hadron scattering.

Earlier we noted that the s - and t -channel diagrams for MM scattering may be continuously deformed into one another. It is often supposed that quark-exchange diagrams are merely another way of modeling t -channel meson exchange, but we argue that this assertion is not correct by considering a deformation of the quark-exchange diagram [Fig. 1(c)] that looks like a particular type of t -channel meson exchange [Fig. 1(d)]. This diagram results from scattering the exchanged quark backwards and then forwards in time, and requires the introduction of additional $q\bar{q}$ -annihilation and creation operators into the Hamiltonian. In Fig. 1(d) we have an intermediate state with six quark lines, but in Fig. 1(a) we can cut the diagram and have only two lines [7]. Hence quark-exchange processes may look like t -channel meson-exchange processes, but they cannot look like s -channel resonance processes and must therefore represent new physics beyond the usual s - t duality.

In our earlier papers on this subject we described how we used the nonrelativistic quark model to calculate effective potentials based on quark exchange. The Hamiltonian used in those calculations is a simplified version of the quark-model Hamiltonian used in calculations of the spectroscopy and decays of mesons and baryons [8,9], as well as the properties of the deuteron [10], thus leading to a unified description of both stationary $q\bar{q}$ and scattering hadron states from a single model. Here we review the physics underlying scattering systems based on s -channel meson resonances and quark-exchange dynamics in a coupled-channel Schrödinger picture. It turns out that, at the present levels of experimental and theoretical accuracy, no contributions from t -channel meson exchange are required.

AN APPLICATION TO S-WAVE PSEUDOSCALAR-PSEUDOSCALAR SCATTERING

An incoming $I=0$ $\pi^+\pi^-$ scattering state, for example, may scatter through an s -channel meson resonance via $q\bar{q}$ -annihilation and creation or through a quark-exchange process into an outgoing asymptotic $\eta\eta$ (or $\eta\eta'$ or $\eta'\eta'$) state if the $\pi\pi$ invariant mass exceeds the appropriate threshold. This same initial state may also scatter into a K^+K^- final state via an s -channel resonance if the creation vertex [Fig. 1(b)] produces an $s\bar{s}$ pair.

A $\pi\pi$ state below $\eta\eta$ threshold may also scatter via quark exchange into a virtual $\eta\eta$ state, and the amplitude for this process increases if there is an attractive $\eta\eta$ potential near the origin which effectively lowers the threshold. (Here and below we use η as a generic label for either an η or η' state.) Because of strong mixing between the $(u\bar{u} + d\bar{d})/\sqrt{2}$ and $s\bar{s}$ components of the physical η , this virtual state may make a transition to a $qq\bar{q}\bar{q}$ MM state with one $q\bar{q}$ pair being an $s\bar{s}$ pair. A second quark-exchange scattering can then complete an indirect second-order transition from $I=0$ $\pi\pi$ to $K\bar{K}$. This process is known to play an essential role in the dynamics of such systems in our coupled-channel model, as discussed in Refs. [2] and [3] and below. Thus we see that a complete description of these scattering processes requires a coupled-channel approach, and that the $\eta\eta$ (and $\eta\eta'$ and $\eta'\eta'$) channels are potentially important even at energies where they are virtual processes.

A reasonable starting point for S -wave PP scattering is the radial coupled-channel matrix Schrödinger equation

$$(\underline{K} + \underline{M} + \underline{V})\mathbf{u}_{I,S}(r) = E\mathbf{u}_{I,S}(r). \quad (1)$$

Here the radial wave function $\mathbf{u}_{I,S}(r)$ represents the amplitude for two mesons or a $q\bar{q}$ system with net isospin I and strangeness S to have relative separation r . In Eq. (1), \underline{K} is a diagonal nonrelativistic kinetic energy operator, and \underline{M} is a diagonal mass matrix, so that E is the total nonrelativistic energy and not simply the kinetic energy. The nondiagonal potential matrix \underline{V} contains three different types of entries which correspond to three distinct physical processes: $P_1P_2 \leftrightarrow P'_1P'_2$ of Fig. 1(c), and $P_1P_2 \leftrightarrow S$ and $S \leftrightarrow S$, which are the components of Fig. 1(b) (where P_i represents a pseudoscalar and S a scalar meson).

We have determined the $P_1P_2 \leftrightarrow P'_1P'_2$ potentials from a variational nonrelativistic quark-model calculation which concluded that the $qq\bar{q}\bar{q}$ low-lying states are mainly scattering states of 0^-0^- meson pairs (with a numerically insignificant 1^-1^- component) and that intermeson "nuclear" forces have a significant contribution arising from quark-exchange processes driven by, in the PP sector, the hyperfine interaction [2,3]. One parameter in our previous analysis was chosen from a fit of the $I=2$ $\pi\pi$ S -wave phase shift to data [11] and is discussed below, while the remaining parameters were determined by low-energy meson spectroscopy.

The range of the quark-exchange potentials is largely determined by the meson radii, and, as we believed that

the quark model underestimated the experimentally-determined meson radii by a factor of about 2, we previously [1–3] allowed ourselves the freedom to double the range of each extracted meson-meson potential, and then scaled each of their strengths by a common factor (determined to be 0.5) from a fit to the $I=2$ $\pi\pi$ phase-shift data [2]. We then converted these potentials to equivalent square-well potentials with similar low-energy single-channel phase shifts and ranges of 0.8 fm to solve the coupled-channel Schrödinger equation numerically. The discrepancy in the π radius may, however, be caused by vector-meson dominance (VMD) which would make its measured electromagnetic radius a convolution of the π and ρ radii. If this is the case, then our argument for expanding the range of the potentials is suspect.

The recent results of Barnes and Swanson [5] show that the extracted $\pi\pi$ potentials require significant modification, but suggest that non- π potentials do not. They arrive at this conclusion because their direct calculation of the phase shift from the Born-level matrix element for PP scattering, and the phase shifts generated by scattering mesons through the effective threshold potential (found by taking the Fourier transform of the Born-scattering matrix element), differ significantly for $\pi\pi$ scattering but not for KK scattering. This suggests that our rescaling of the effective potentials is required because the π mass is small, and not because the meson radii are underestimated. This in turn suggests that future work on potential models might profitably attempt to make contact with chiral dynamics which successfully describes low-momentum pseudoscalar dynamics [16,18]. In the next section we will discuss the effect of this observation on our earlier $I=0, \frac{1}{2}$, and 1 coupled-channel results and, for the moment, continue with our review of the model.

The $P_1 P_2 \leftrightarrow S$ potentials which determine to the vertex

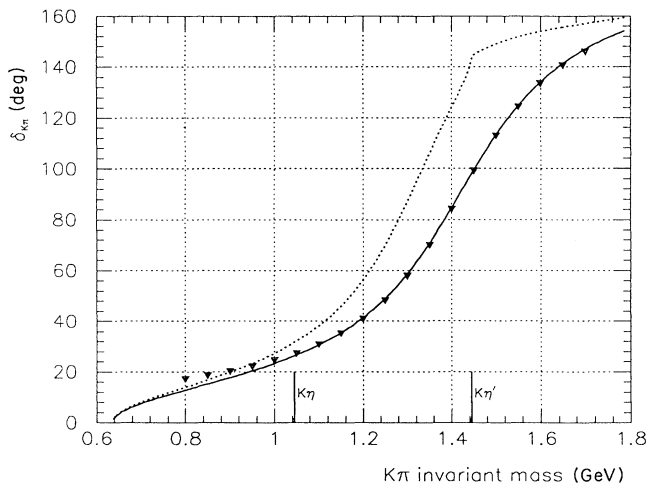


FIG. 2. The S -wave phase shifts for $K\pi \rightarrow \kappa \rightarrow K\pi$ scattering through a Breit-Wigner s -channel interaction (triangles), and through two-channel (solid line) and four-channel (dotted line) Schrödinger equations with no quark-exchange interactions. $K\eta$ and $K\eta'$ thresholds are marked with vertical lines.

factors in Fig. 1(b) are calculated from an SU(3)-symmetric 3P_0 $q\bar{q}$ annihilation picture which includes Clebsch-Gordan factors dependent on the $P_1 P_2$ flavor wave functions, mass-dependent form factors, and an overall square-well depth chosen to reproduce the quark model $f_0(1300) \rightarrow \pi\pi$ width [9].

The $S \leftrightarrow S$ potential, which allows the $q\bar{q}$ resonance to propagate from one vertex to the other in Fig. 1(b), consists of a repulsive $1/r^2$ P -wave centrifugal barrier, a deep square-well $q\bar{q}$ confining potential (normally taken to be 10 GeV) with an interior depth (for $r < 0.8$ fm) chosen to reproduce the ground-state 3P_0 masses in agreement with both experiment and the predictions of the quark model [8].

The dimensions of the matrices in Eq. (1) are determined by the number of S -wave pseudoscalar pairs and scalar $q\bar{q}$ mesons in the flavor sector being investigated. The wave functions $\mathbf{u}_{I,S}$ are of the form

$$\mathbf{u}_{1,2} = (u_{KK}), \quad \mathbf{u}_{3/2,1} = (u_{K\pi I=3/2}), \quad \mathbf{u}_{1/2,1} = \begin{pmatrix} u_{K\pi I=1/2} \\ u_{K\eta} \\ u_{K\eta'} \\ u_{K_0^*(1410)} \end{pmatrix}, \quad (2)$$

$$\mathbf{u}_{1,0} = \begin{pmatrix} u_{n\pi} \\ u_{K\bar{K} I=1} \\ u_{\eta'\pi} \\ u_{a_0(1300)} \end{pmatrix}, \quad \mathbf{u}_{0,0} = \begin{pmatrix} u_{\pi\pi I=0} \\ u_{K\bar{K} I=0} \\ u_{\eta\eta} \\ u_{\eta\eta'} \\ u_{\eta'\eta'} \\ u_{f_0(1300)} \\ u_{f_0'(1500)} \end{pmatrix},$$

or

$$\mathbf{u}_{2,0} = (u_{\pi\pi I=2}).$$

We solve Eq. (1) numerically to determine these scattering-state wave functions; their asymptotic behavior yields the energy-dependent phase shifts, and the inelasticities are found by comparing the relative amplitudes of outgoing waves in each channel for a given incoming wave.

This model can be related to the standard picture for Breit-Wigner scattering through an s -channel resonance of mass m_R and width Γ_R by considering a two-channel problem in which the incoming PP system, channel 1, scatters through annihilation to the resonance, channel 2 [Fig. 1(b)] [12]. There are no quark-exchange effects in the Breit-Wigner model, so in our model this corresponds to $V(\text{PP} \rightarrow \text{PP}) = 0$ but $V(\text{PP} \rightarrow S)$ and $V(S \rightarrow S) \neq 0$. In Fig. 2 we compare the S -wave Breit-Wigner phase shift for $K\pi \rightarrow \kappa \rightarrow K\pi$ at invariant energy E :

$$\delta_{\text{BW}}^S = \arctan \left[\frac{\frac{1}{2}\Gamma_\kappa}{m_\kappa - E} \right], \quad (3)$$

with $m_\kappa = 1.42$ GeV and $\Gamma_\kappa = 0.38$ GeV (shown as invert-

ed triangles) to the two-channel phase shift (shown as a solid line) with $m_\kappa = 1.47$ and $V_{\kappa \rightarrow K\pi} = 0.41 \oplus (0.8 \text{ fm} - r)$ GeV by solving Eq. (1) numerically. We see that the two phase shifts agree numerically except at low energies where the Breit-Wigner model does not take into account the $K\pi$ threshold. Note that the underlying resonance masses are not equal [3]. We conclude that our coupled-channel model leads to the standard Breit-Wigner results in the appropriate two-channel limit where there are only s -channel resonance interactions.

Shown as a dotted line in Fig. 2 is the phase shift resulting when the s -channel κ is also coupled to $K\eta$ and $K\eta'$ intermediate states corresponding to a four-channel Schrödinger equation. Note that this $K\pi$ phase shift differs markedly from the Breit-Wigner model, and is affected by the additional couplings even below the $K\eta$ and $K\eta'$ thresholds where these channels are virtual.

We have presented the results found when Eq. (1) is solved numerically in the $I=0, 1, 2$ nonstrange sectors and the $I=1/2$ and $3/2$ strangeness ± 1 sectors when all meson-meson potentials are rescaled [2,3]. We also found that these solutions were not extremely sensitive to the parameter set we chose for these three sets of potentials.

A comparison of the predictions of this model with experimental data has led to many insights into the behavior of these systems and the possible resolution of several outstanding problems in hadron physics. A list of successes includes an understanding of the masses, widths, and branching fractions of the S^* and δ [now called the $f_0(975)$ and $a_0(980)$ respectively] scalars and the $q\bar{q}$ scalar mesons, low-energy PP phase shifts [2,3], the two-photon widths of the S^* and δ [13], the $\Delta I=1/2$ rule in K decay [14], PP-invariant mass distributions in $J/\psi \rightarrow P_1 P_2 V$ [15], and the physical origins of backgrounds [3].

A REANALYSIS OF THE COUPLED-CHANNEL PHASE SHIFTS

Given the wide-ranging claims for the model summarized in the above paragraph, and the recent results of Barnes and Swanson which suggests that only the $\pi\pi$ potentials require significant rescaling, it is appropriate to recalculate the coupled-channel results.

It is interesting to note first that some evidence supporting the conclusion of Barnes and Swanson comes from our extracted PP potentials. The S -wave $I=2$ $\pi\pi$ scattering length $a_0^I m_\pi / \hbar$, where a_0^I (I denoting isospin) is determined from

$$a_0^I = \lim_{k \rightarrow 0} \frac{\arctan(\delta_0^I)}{k}, \quad (4)$$

is predicted to be -0.06 by Weinberg [16], and by Morgan and Pennington [17], and -0.059 fm by Barnes and Swanson [5]. In our quark model this scattering length is -0.05 , in good agreement with the above results, before rescaling the potential, but -0.18 after rescaling. In chiral-perturbation theory with resonance exchange a_0^2 is calculated to be -0.043 [18], while the empirical result is -0.028 ± 0.012 [18,19]. Consistency with these results

therefore supports the hypothesis that rescaling is required to increase the effect of the $\pi\pi$ potentials, which are extracted from a variational calculation of the $\pi\pi$ ground state, on scattering systems at energies well above threshold; near threshold the extracted potentials give better results.

In the $I=0$ sector, however, our results do not agree so closely with Weinberg's predicted scattering length of 0.20, or with the chiral perturbation theory prediction of 0.21. The single-channel scattering of a $\pi\pi$ system through the extracted $\pi\pi$ potential gives $a_0^0 m_\pi / \hbar = 0.08$ before rescaling and 0.39 after rescaling (see below for the values of these potentials). In coupled-channel scattering we calculate a scattering length of 0.47 before rescaling any of the meson-meson potentials, and, with only the $\pi\pi \rightarrow \pi\pi$ potential rescaled, 0.77. Without the quark-exchange potentials, the PP couplings to the f_0 scalar meson alone lead to a $\pi\pi$ scattering length of 0.36. An experimental measurement of this scattering length using the K_{e4} decay, $K \rightarrow \pi^+ \pi^- e^+ \nu$, finds 0.28 ± 0.05 in one approach and 0.36 ± 0.11 in another [20]. These results demonstrate the strong effect of the virtual PP and scalar channels in the $I=0$ multichannel solution all the way down to $\pi\pi$ threshold, and that rescaling is required mainly to compensate for a momentum dependence not included in our threshold potentials.

These conclusions are also supported by results in the $I=1/2$ and $3/2$ $K\pi$ scattering sectors. In $I=3/2$ we find a scattering length, now defined as a dimensionless number times $1/m_\pi$:

$$a_0^{1/2,3/2} = \frac{m_\pi + \delta_0^{1/2,3/2}}{\sqrt{(\sqrt{s} - m_K - m_\pi) 2m_K m_\pi / (m_K + m_\pi)}}, \quad (4')$$

of -0.07 for unrescaled potentials and -0.18 for rescaled potentials. The chiral result is -0.06 and the experimental results lie in the range -0.13 to -0.05 [21]. We find $a_0^{1/2}$ to be 0.16 with K^* exchange alone, 0.26 with all PP potentials unrescaled, and 0.42 with potentials involving a π being rescaled. The chiral result is 0.19 and the experimental data range from 0.13 to 0.24, showing that our best agreement for these threshold measurements comes when we do not rescale any potentials.

One might ask why the threshold results do not obviate the need for any rescaling of our extracted PP potentials. However, since we wish to describe data from the thresholds to about 1.5 GeV, well beyond the viability of the chiral approach, we have opted for a more global approach and have rescaled those potentials involving pions, as suggested by the results of Barnes and Swanson.

We have recalculated for seven-channel $I=0$ $\pi\pi$, four-channel $I=1/2$ $K\pi$, and four-channel $I=1$ $\pi\eta$ elastic phase shifts in the square-well approximation by replacing the extracted potentials with equivalent square-well potentials which give approximately the same low-energy phase shifts in a single-channel scattering approximation. These new equivalent potentials are 0.8 fm wide and have

strengths of $V_u^e = +0.15$, $V_k^e = +0.105$, $V_s^e = +0.07$, $V_u^c = -0.16$, $V_k^c = -0.11$, and $V_s^c = -0.06$ GeV. They may be compared with our earlier rescaled equivalent potentials of $V_u^e = +0.57$, $V_k^e = +0.29$, $V_s^e = +0.18$, $V_u^c = -0.43$, $V_k^c = -0.43$, and $V_s^c = -0.15$ GeV and the same range. Here the superscript e or c refers to the symmetry of the flavor wave function of the diquark and anti-diquark pairs; they are either “cryptoexotic” $\bar{3} \otimes 3$ (V^c) as ordinary $q\bar{q}$ mesons or they are “exotic” $6 \otimes \bar{6}$ (V^e) [22]. The subscripts refer to the mass of the quarks which are used to calculate the SU(3) symmetric potentials, V_u for $uu\bar{u}\bar{u}$ (with u generic for u and d), V_k for $us\bar{u}\bar{s}$, and V_s for $ss\bar{s}\bar{s}$ systems. We use u - and s -quark masses of 0.375 and 0.600 GeV respectively and take the average mass for the “ k ” quark. For the $I = \frac{1}{2}$ $K\pi/K\eta/K\eta'$ system we use average potentials, and use the old rescaled $V_u^{(c,e)}$ potentials only when pions are involved. A more detailed background to this procedure may be found in Refs. [2] and [3].

In Figs. 3, 4, and 5, we show the elastic $I=0, \frac{1}{2}$, and 1 phase shifts of the light PP pair scattering through the old potentials (solid lines), and the new potentials where only those potentials involving pions are rescaled (dashed lines). Note that the overall features of the phase shifts have remained unchanged. We also show the phase shifts which result when the quark-exchange forces are set equal to zero (dotted lines) and discuss them below. We know from the exotic sectors, where $q\bar{q}$ annihilation is not allowed, that quark exchange represents the data quite well, so we expect these forces to be important here.

We have not tuned parameters to show that, for exam-

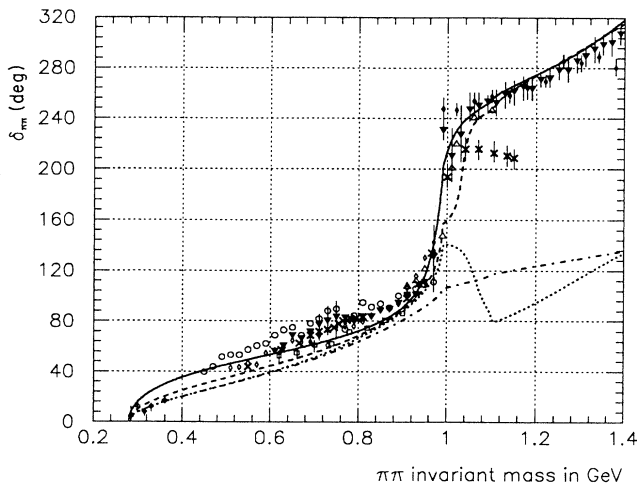


FIG. 3. The elastic S -wave phase shifts for $I=0$ $\pi\pi$ scattering with all potentials rescaled (solid line), with only $V_{\pi\pi}^{I=0}$ rescaled (dashed line), with all quark-exchange potentials turned off (dotted line), and with all quark-exchange potentials and couplings to the $f_0'(1500)$ turned off (dot-dashed line). Most of the points come from different analyses of the same data by Grayer *et al.* [24]; however, the points marked with “ \times ”s are from Protopopescu *et al.* [25] and the five points at low energy come from Rossetet *et al.* [20].

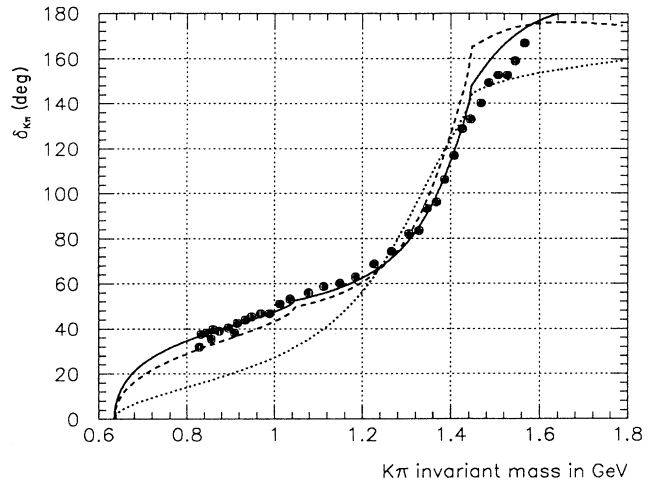


FIG. 4. The elastic S -wave phase shifts for $I = \frac{1}{2}$ $K\pi$ scattering with all potentials rescaled (solid line), with only the quark-exchange potentials involving pions rescaled (dashed line), and with all quark-exchange potentials turned off (dotted line). The data is from the experiment of Aston *et al.* [26].

ple, agreement with the measured masses and widths of the $S^*(980)$ and $\delta(975)$ can be achieved. Such agreement would be much more meaningful if the actual extracted potentials were used rather than the equivalent square-well potentials [23]. An even better model would be to incorporate the Born-approximation calculation directly into a coupled-channel framework with all $q\bar{q}$ -resonance channels and PP states included, although it is not yet clear that this is possible. Here we simply demonstrate that the essential predictions of the quark-exchange

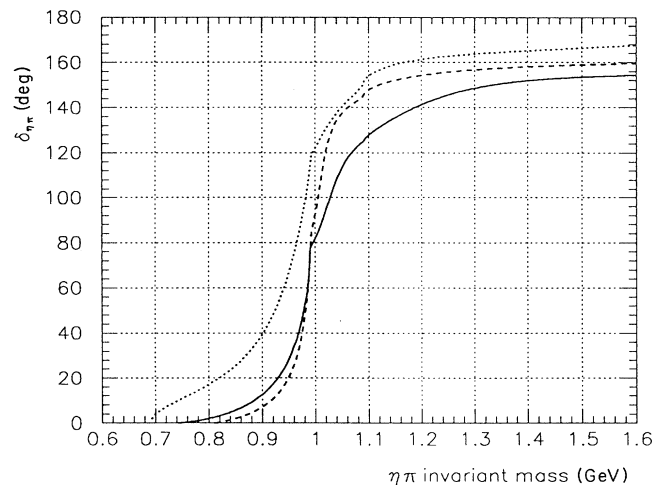


FIG. 5. The elastic S -wave phase shifts for $I=1$ $\eta\pi$ scattering with all potentials rescaled (solid line), with only the quark-exchange potentials involving pions rescaled (dashed line), and with all quark-exchange potentials turned off (dotted line).

coupled-channel model are not lost when we restrict our rescaling of the underlying potentials to the π sectors.

In $I=0$ (Fig. 3) we see that the phase shifts found by scattering with all rescaled quark-exchange potentials (solid line), and with only rescaled $\pi\pi \rightarrow \pi\pi$ quark-exchange potentials (dashed line), plus, in both cases, s -channel resonance processes, are quite similar to each other, and both offer reasonable representations of the data [20,24,25]. An argument could be made that the phase shift found by rescaling only the $\pi\pi$ potential is favored by the low-energy data of Rosselet *et al.* [20]. In $I=0$ (Fig. 3) we see that the phase shift found when the quark-exchange forces are turned off (dotted line) differs significantly in the S^* region from the phase shifts found by including both quark-exchange and s -channel resonance processes. The behavior of this s -channel-driven phase shift at $K\bar{K}$ threshold results from the transition matrix leaving the unitary circle and crossing below the center of the Argand circle. No choice of parameters produces a phase shift that continues to rise through $K\bar{K}$ threshold. The peculiar behavior around $K\bar{K}$ threshold is due to an interference effect between the $f'_0(1500)$ and the $f_0(1300)$, as can be seen from the phase shift found when both quark exchange and f'_0 couplings are turned off (dot-dashed line). This demonstrates that the quark-exchange forces are essential, at least in this coupled-channel Schrödinger picture, to obtain agreement with known data.

The effect of the quark-exchange potentials is not so dramatic in the $I=1/2$ channel (Fig. 4). We have previously discussed, however, that the phase shift with quark-exchange forces (solid line) gives a much better representation of the data [26], especially at low $K\pi$ invariant mass, than the pure s -channel resonance-driven interaction (dotted line) [3]. As this figure also demonstrates, the phase shift with only quark-interaction potentials involving pions rescaled (dashed line) is in good qualitative agreement with the earlier results and the data.

When only the exchange potentials involving pions are rescaled the resulting $I=1$ $\eta\pi$ phase shift (not shown) falls at $K\bar{K}$ threshold. However, if the $q\bar{q}$ -confinement potential for the $a_0(1300)$ is reduced from 10 GeV to 5 GeV the resulting T matrix crosses the Argand diagram above the center, and the phase shift (the dashed line in Fig. 5) is similar to the phase shift with all rescaled potentials (solid line) but suggests a $\delta(980)$ width of about 25 MeV rather than the measured value of 57 ± 11 MeV. The phase shift with no quark-exchange potentials (dotted line) leads to a “ δ ” effect which is lighter and much wider than measured; the quark-exchange forces “unbind” the δ . This happens because the quark-exchange forces in this sector are repulsive near threshold, for example the $\eta\pi \rightarrow \eta\pi$ potential is 0.28 GeV high and 0.8 fm wide. This behavior is very different from the $I=0$ sector where they are attractive and increase the $\pi\pi$ elastic phase shift. An experimental determination of low-energy $\eta\pi$ phase shifts would test this predicted threshold behavior.

We now discuss whether the $a_0(1300)$ is a $q\bar{q}$ state or a $K\bar{K}$ molecule. Fig. 6 shows several $\eta\pi$ elastic phase shifts

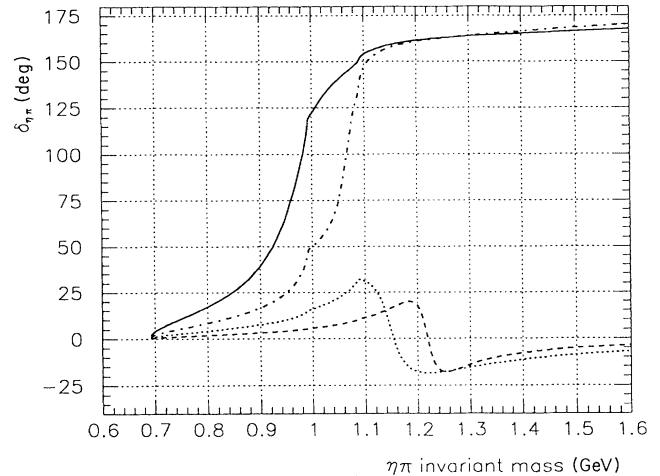


FIG. 6. The elastic S -wave phase shifts for $I=1$ $\eta\pi$ scattering with all quark-exchange potentials turned off and with various couplings of the asymptotic PP states to the $a_0(1300)$. The solid line corresponds to an a_0 width in two-channel $\eta\pi \rightarrow a_0 \rightarrow \eta\pi$ scattering of about 300 MeV, the dot-dashed line to about 200 MeV, the dotted line to about 120 MeV, and the dashed line to about 50 MeV.

due to s -channel resonance scattering alone with different overall $P_1 P_2 a_0$ vertex strengths. In two-channel $\eta\pi \rightarrow a_0 \rightarrow \eta\pi$ scattering (not shown) the widths of the resonances in Fig. 6 are 50 MeV (dashed line), 120 MeV (dotted line), 200 MeV (dot-dashed line) and 300 MeV (solid line). The multichannel solution in the narrow

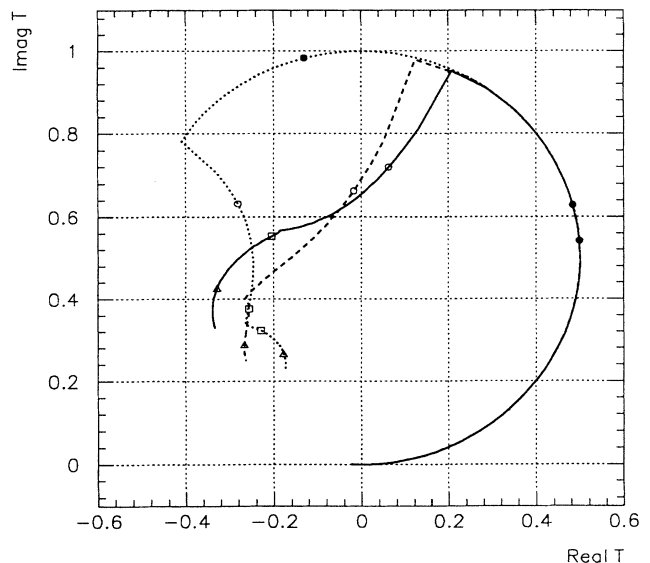


FIG. 7. The T -matrix element for S -wave $I=1$ $\eta\pi$ scattering with all potentials rescaled (solid line), with only the quark-exchange potentials involving pions rescaled (dashed line), and with all quark-exchange potentials turned off (dotted line). The solid circles indicate 0.98 GeV, the open circles 1.00 GeV, the squares 1.10 GeV, the triangles 1.20 GeV, and the curves end at 1.30 GeV.

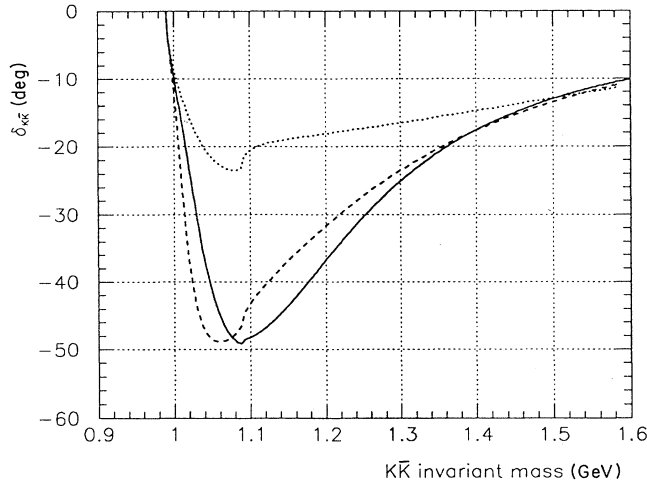


FIG. 8. The elastic S -wave phase shifts for $I=1$ $K\bar{K}$ scattering with all potentials rescaled (solid line), with only the quark-exchange potentials involving pions rescaled (dashed line), and with all quark-exchange potentials turned off (dotted line).

width case (dashed line) corresponds to a loop in the Argand circle which crosses the imaginary axis below the center (because the inelasticity η is less than 0.5) and leads to a falling phase shift on resonance. As the coupling to the a_0 is increased, the phase shift rises through the resonance, and the mass of the $a_0(1300)$ falls below $K\bar{K}$ threshold. One may be tempted to conclude from this that the δ is the $a_0(1300)$ $q\bar{q}$ quark-model state whose mass and width have been highly altered by multichannel effects. The Argand diagram (Fig. 7) for the solutions with quark-exchange effects, however, is very inelastic just above $K\bar{K}$ threshold, and the $K\bar{K}$ elastic phase shift (Fig. 8) drops at threshold, indicating that the δ has a large $K\bar{K}$ component, a structure far removed from a simple $q\bar{q}$ -meson resonance.

To obtain reliable quantitative results it is important to improve upon the square-well approximation by solving the coupled-channels equation with either actual extracted potentials or with potentials that reproduce the Born approximation phase shifts [23].

RESULTS FOR KK SCATTERING

The last PP S -wave system to study in this model is the $I=1$ strangeness ± 2 spanned by the states K^+K^+ , $(K^+K^0+K^0K^+)/\sqrt{2}$, K^0K^0 and their Hermitian conjugates. There are no strangeness ± 2 $q\bar{q}$ states which can be produced as s -channel resonances, so these mesons interact only through quark-exchange processes in this model. In other models one may have t -channel meson exchange or s -channel $qq\bar{q}\bar{q}$ resonances driving these reactions. Also note that we do not consider the $I=0$ $(K^+K^0-K^0K^+)/\sqrt{2}$ system and its Hermitian conjugate, as they are antisymmetric in flavor and must be in at least a relative P wave.

As discussed above, our extraction of the $us\bar{u}\bar{s}$ potential predicts a repulsive potential for the exotic KK chan-

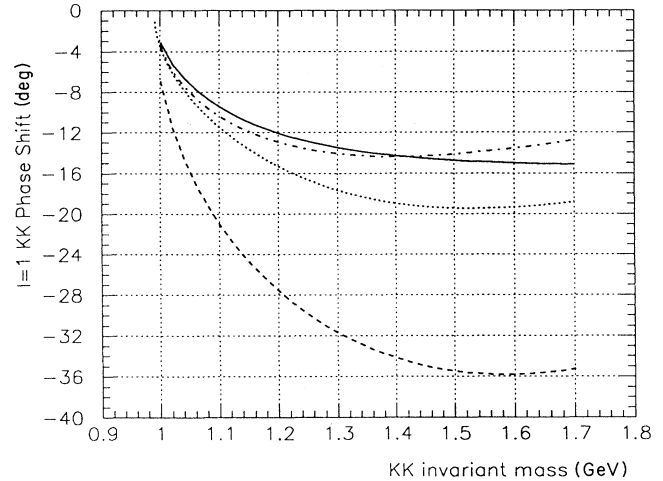


FIG. 9. $I=1$ strangeness ± 2 KK elastic scattering S -wave phase shifts for scattering through the potential-model-extracted potential (solid line), for its equivalent square-well potential (dot-dashed line), for the rescaled extracted potential (dashed line), and for the Born phase shift (dotted line) [5].

nel. In the above approximations this potential is replaced by an equivalent square-well potential with $V_k^e = V_{KK} = +0.11$ or $+0.29$ GeV for the extracted and rescaled potentials respectively, and a range of $a = 0.8$ fm in each case. In Fig. 9 we show the strangeness ± 2 KK S -wave scattering phase shifts as a function of the KK nonrelativistic energy $E = T + 2m_K$, where T is the kinetic energy, for the actual extracted KK potential (solid line), for the square-well approximation to this potential (dot-dashed line), and for the rescaled KK potential (dashed line). We show all of these curves for complete-

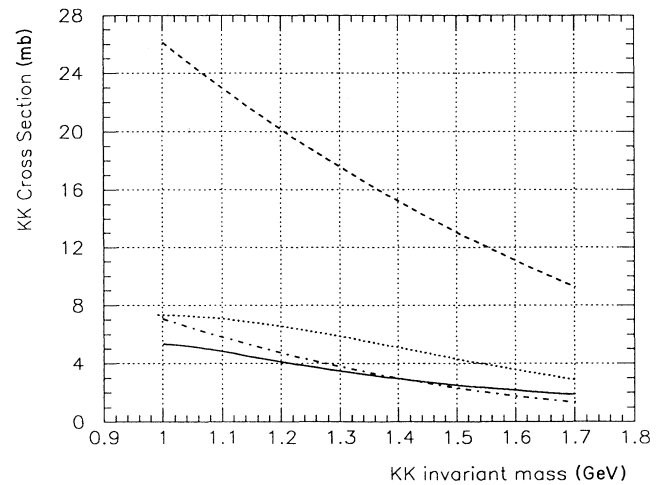


FIG. 10. The $I=1$ strangeness ± 2 KK elastic cross section for S -wave scattering through the potential-model-extracted potential (solid line), for its equivalent square-well potential (dot-dashed line), for the rescaled extracted potential (dashed line), and for the Born phase shift (dotted line) [5].

ness; the predictions of the model are those generated by scattering through the actual extracted potential (solid line). The square-well phase shift is found by solving Eq. (1) numerically or, equivalently, from

$$\delta_{KK}^S = \begin{cases} \arctan[(k/\kappa) \tanh(\kappa a)] - ka, & T < V, \\ \arctan[(k/\kappa) \tan(\kappa a)] - ka, & T > V, \end{cases} \quad (5)$$

where $k = \sqrt{2\mu T}/\hbar$, $\kappa = \sqrt{2\mu|T-V|}/\hbar$, and $\mu = 0.5m_K$. The other phase shifts are found by numerical integration of Eq. (1). The Born-approximation results of Barnes and Swanson are shown as the dotted line, which agrees with the quark-model calculation at the 30% level. These phase shifts can be converted into the S -wave cross-section predictions shown in Fig. 10 through

$$\delta_{KK}^S = \frac{8\pi}{k^2} \sin^2(\delta_{KK}^S), \quad (6)$$

and lead to threshold cross sections of 5.3, 7.1, and 58 mb for the actual (solid), equivalent square-well (dot-dashed), and stretched (dashed) potentials respectively. The threshold cross section reported by Barnes and Swanson in the Born approximation is 7.3 mb, and their cross section, with nonrelativistic kinematics, is shown as a dotted line. The quark-model scattering-length predictions are -0.15 , -0.17 , and -0.49 fm respectively, while the Born approximation predicts -0.17 fm.

An experimental measurement of these quantities would be a useful test of the quark-exchange model, and

accurate data may help resolve issues regarding the re-scaling of the non- π potentials.

CONCLUSIONS

We have discussed possible mechanisms for the interaction of scattering hadrons and conclude from both general arguments and a specific calculation in the S -wave PP scattering systems that the interaction is dominated by s -channel resonance production and quark-exchange effects; t -channel meson exchange is not yet required to fit the data at this accuracy. In this sector quark exchange leads to the binding of $\overline{K}K$ states within the framework of a matrix Schrödinger equation. As discussed elsewhere, this interpretation appears to solve many problems in light-hadron physics. We have also presented the phase-shift, scattering-length and cross-section predictions of the quark-exchange meson-meson scattering model to the $I=1$ strangeness ± 2 $\overline{K}K$ and $\overline{K}K$ sectors. We find a repulsive $\overline{K}K$ interaction and show the resulting elastic phase shift and cross-section predictions which are similar to the Born-approximation results.

ACKNOWLEDGMENTS

I would like to thank Ted Barnes and Nathan Isgur for many useful discussions and contributions. This work was partially supported by the U.S. Department of Energy, Division of High Energy Physics, under Contract Number DE-FG05-91ER40622, and the Texas National Research Laboratory Commission.

-
- [1] J. Weinstein and N. Isgur, Phys. Rev. Lett. **48**, 659 (1982); Phys. Rev. D **27**, 588 (1983).
 - [2] J. Weinstein and N. Isgur, Phys. Rev. D **41**, 2236 (1990).
 - [3] J. Weinstein and N. Isgur, Phys. Rev. D **43**, 95 (1991).
 - [4] K. Dooley, E. S. Swanson, and T. Barnes, Phys. Lett. B **275**, 478 (1992).
 - [5] T. Barnes and E. S. Swanson, Phys. Rev. D **46**, 131 (1992).
 - [6] H. Yukawa, Proc. Phys. Math. Soc. Jpn. **17**, 48 (1935).
 - [7] N. Isgur, Acta Phys. Austriaca Suppl. **XXVII**, 177 (1985).
 - [8] S. Godfrey and N. Isgur, Phys. Rev. D **32**, 189 (1985).
 - [9] R. Kokoski and N. Isgur, Phys. Rev. D **35**, 907 (1987); Phys. Rev. Lett. **44**, 869 (1985).
 - [10] K. Maltman and N. Isgur, Phys. Rev. D **29**, 952 (1984).
 - [11] F. Wagner, in *Proceedings of the XVII International Conference on High Energy Physics*, London, England, 1974, edited by J. R. Smith (Rutherford High Energy Laboratory, Didcot, 1975); W. Hoogland *et al.*, Nucl. Phys. **B126**, 109 (1977).
 - [12] J. Weinstein, in *The Hadron Mass Spectrum*, Proceedings of the Conference, St. Goar, Germany, 1990, edited by E. Klempt and K. Peters [Nucl. Phys. B (Proc. Suppl.) **21**, 207 (1991)].
 - [13] T. Barnes, Phys. Lett. **165B**, 434 (1985).
 - [14] N. Isgur, K. Maltman, J. Weinstein, and T. Barnes, Phys. Rev. Lett. **64**, 161 (1990).
 - [15] J. Weinstein, in *Proceedings of the Tau-Charm Factory Workshop*, Stanford, California, 1989, edited by L. V. Beers (SLAC Report No. 343, Stanford, 1989); in *Hadron 89*, Proceedings of the International Conference on Hadron Spectroscopy, Corsica, France, 1989, edited by F. Binon, J.-M. Frère, and J.-P. Peigneux (Edition Frontières, Gif-sur-yvette, France 1989).
 - [16] S. Weinberg, Phys. Rev. Lett. **17**, 616 (1966).
 - [17] M. Pennington (private communication).
 - [18] J. Gasser *et al.*, Ann. Phys. (N.Y.) **158**, 142 (1984); J. F. Donoghue *et al.*, Phys. Rev. D **38**, 2195 (1988); V. Bernard *et al.*, Nucl. Phys. **B364**, 283 (1991); Phys. Rev. D **43**, R2757 (1991); **44**, 3698 (1991).
 - [19] J. L. Petersen, CERN Yellow Report No. 77-04, 1977 (unpublished).
 - [20] L. Rosset *et al.*, Phys. Rev. D **15**, 574 (1977).
 - [21] O. Drumbaj *et al.*, Nucl. Phys. **B216**, 277 (1983); M. J. Matison *et al.*, Phys. Rev. D **9**, 1872 (1974); C. B. Lang, Nuovo Cimento A **41**, 73 (1977); N. O. Johannesson and J. L. Petersen, Nucl. Phys. **B68**, 397 (1973); A. Karabouraris and G. Shaw, J. Phys. G **6**, 583 (1980).
 - [22] R. L. Jaffe, Phys. Rev. D **15**, 267 (1977); **15**, 281 (1977).
 - [23] J. Weinstein (in preparation).
 - [24] G. Grayer *et al.*, Nucl. Phys. **B75**, 189 (1974).
 - [25] S. Protopopescu *et al.*, Phys. Rev. D **7**, 1280 (1973).
 - [26] D. Aston *et al.*, Nucl. Phys. **B296**, 493 (1988).